



Contents lists available at ScienceDirect

## Journal for Nature Conservation

journal homepage: [www.elsevier.de/jnc](http://www.elsevier.de/jnc)

## Differentiating geological fertility derived vegetation zones in Kruger National Park, South Africa, using Landsat and MODIS imagery

Christopher Munyati<sup>a,\*</sup>, Thihanedzwi Ratshibvumo<sup>b,1</sup>

<sup>a</sup> Ecosystems Earth Observation Research Group, Natural Resources and the Environment Unit, Council for Scientific and Industrial Research, P.O. Box 395, Pretoria 0001, South Africa

<sup>b</sup> Department of Ecology and Resource Management, School of Environmental Sciences, University of Venda, Private Bag X5050, Thohoyandou 0950, South Africa

## ARTICLE INFO

## Article history:

Received 15 May 2008

Accepted 10 August 2009

## Keywords:

biodiversity conservation  
habitat mapping  
remote sensing  
soil fertility

## ABSTRACT

Spatial technologies present possibilities for producing frequently updated and accurate habitat maps, which are important in biodiversity conservation. Assemblages of vegetation are equivalent to habitats. This study examined the use of satellite imagery in vegetation differentiation in South Africa's Kruger National Park (KNP). A vegetation classification scheme based on dominant tree species but also related to the park's geology was tested, the geology generally consisting of high and low fertility lithology. Currently available multispectral satellite imagery is broadly either of high spatial but low temporal resolution or low spatial but high temporal resolution. Landsat TM/ETM+ and MODIS images were used to represent these broad categories. Rain season dates were selected as the period when discrimination between key habitats in KNP is most likely to be successful. Principal Component Analysis enhanced vegetated areas on the Landsat images, while NDVI vegetation enhancement was employed on the MODIS image. The images were classified into six field sampling derived classes depicting a vegetation density and phenology gradient, with high (about 89%) indicative classification accuracy. The results indicate that, using image processing procedures that enhance vegetation density, image classification can be used to map the park's vegetation at the high versus low geological fertility zone level, to accuracies above 80% on high spatial resolution imagery and slightly lower accuracy on lower spatial resolution imagery. Rainfall just prior to the image date influences herbaceous vegetation and, therefore, success at image scene vegetation mapping, while cloud cover limits image availability. Small scale habitat differentiation using multispectral satellite imagery for large protected savanna areas appears feasible, indicating the potential for use of remote sensing in savanna habitat monitoring. However, factors affecting successful habitat mapping need to be considered. Therefore, adoption of remote sensing in vegetation mapping and monitoring for large protected savanna areas merits consideration by conservation agencies.

© 2009 Elsevier GmbH. All rights reserved.

## Introduction

Updated habitat spatial data are a fundamental requirement in conservation management of the varied biodiversity in protected areas (Mehner et al. 2004; Weiers et al. 2004). The spatial technologies of remote sensing and GIS provide possibilities for production, storage and rapid updating of habitat maps (Lucas et al. 2007; Nagendra 2001; Weiers et al. 2004), given the threats to the stability of habitats from human and natural factors (Bock et al. 2005). For protected areas in tropical and subtropical areas where droughts are frequent, such as Kruger National Park in South Africa, the need for accurate and updated habitat state spatial data is particularly acute. Despite the technology's

capabilities, some of which have been demonstrated in the southern Africa region (e.g. McCarthy et al. 2005; Ringrose et al. 1988, 2003; Verlinden & Masogo 1997) and elsewhere (e.g. Sader et al. 1991) routine use of remote sensing in mapping and monitoring changes in habitats and vegetation types has not been adopted fully by conservation agencies, including in developed countries (Bock et al. 2005; Lucas et al. 2007), and the more expensive and time consuming field surveys (Lucas et al. 2007; Mehner et al. 2004) are still the more common approach. For Kruger National Park (KNP), research utilising parts of the park as a study area has demonstrated the potential role of remote sensing in ecosystem assessments (e.g. Landmann 2003; Mutanga & Skidmore 2004; Mutanga et al. 2004; Verbesselt et al. 2007).

Vegetation assemblages are the equivalent of habitats (Lucas et al. 2007), although terrestrial habitats are generally delineated based on vegetation and topography. Both vegetation and topography are related to geology, the former through the nutrients in the soil from the parent rock material, and the latter through inherent geological resistance to lithospheric-altering

\* Corresponding author. Fax: +27 12 841 4257.

E-mail addresses: [cmunyati@csir.co.za](mailto:cmunyati@csir.co.za) (C. Munyati), [thihanedzwi@yahoo.com](mailto:thihanedzwi@yahoo.com) (T. Ratshibvumo).

<sup>1</sup> Fax: +27 15 962 8594.

agents of weathering, erosion and mass wasting that create various relief features. Whereas it is relatively more challenging to map topography using remotely sensed images, vegetation mapping using images from sensors operating in the visible through to the mid-infrared spectral regions is feasible, depending on the spectral and spatial resolution of the sensor (Lillesand et al. 2004). The mapping and monitoring of habitats has benefited from the technical improvements to sensors on board earth orbiting environmental satellites since the launch of the first satellites, particularly improvements in spectral and spatial resolution.

A number of factors can influence the success of habitat mapping using remotely sensed imagery. The images used should, ideally, be taken at a time of year when discrimination between key habitats is most marked (Lucas et al. 2007). In addition to the spatial and spectral resolution of the sensor, synoptic coverage of large swaths of habitats by satellite images is important for habitats with large spatial extent. Although there is often a trade-off between spatial detail and the need for synoptic coverage of large swaths of habitat (Weiers et al. 2004), use of images from high spatial resolution sensors has been shown to produce more accurate habitat maps (Mehner et al. 2004). The approaches to image processing (supported by ecological knowledge of the area; Bock et al. 2005) are also important for successful habitat mapping by remote sensing. Image classification approaches are commonly used (e.g. Congalton et al. 2002; Mehner et al. 2004; Ringrose et al. 1988, 2003; Sader et al. 1991; Weiers et al. 2004) but their accuracy also depends on the image classification algorithm used, i.e. 'hard classifiers' or the relatively newer soft classifier approaches like spectral mixture analysis (Lillesand et al. 2004). Hard classifiers tend to impose distinct habitat boundaries when in reality zones of intersection between different vegetation types separate the habitats, whereas soft classifiers produce more realistic habitat maps with the percentage of each class found in each pixel (Mehner et al. 2004) but are more complex and require detailed field data. Principal Component Analysis (PCA), a technique for reducing the dimensionality of remotely sensed imagery and thereby increasing the computational efficiency of the classification process (Eklundh & Singh 1993; Lillesand et al. 2004) has been utilised in enhancing images as part of the image classification process (e.g. Call et al. 2003; Conese et al. 1993; Lee et al. 1990). The Normalised Difference Vegetation Index (NDVI), which is based on the high reflectance in the near infrared and absorption in the red spectral ranges by healthy vegetation (Lillesand et al. 2004) is also commonly utilised in vegetation enhancement on images (Kerr & Ostrovsky 2003), NDVI being high (0.3–1) in vegetated areas.

The size and nature (characteristics) of the habitats are also an important factor in accuracy of habitat mapping, irrespective of which image processing algorithms are used. For example, Lucas et al. (2007) have shown that segmentation (rule-based classification) of Landsat ETM+ images gave a good representation of the distribution of habitats (and agricultural land) for the more extensive, contiguous and homogenous habitats that were mapped with accuracies exceeding 80% but accuracies were lower for more complex, broadly defined habitats. Sader et al. (1991) used hard classifiers in classification of Landsat TM imagery to map bird habitat and showed that mature forest habitat could be identified with high accuracy (93%) but classification accuracy for major vegetation succession stages was low.

This research utilised satellite imagery to assess the vegetation (habitat) types of Kruger National Park (KNP) in South Africa. KNP has well established geology-related habitat (vegetation) strata, some based on land systems and others based on vegetation. The aim of the research was to establish the extent to which the geology derived vegetation zones of the park can be reproduced from satellite imagery. The usefulness of such imagery as a source

of updated spatial data on the park's vegetation is then assessed. In terms of spatial and temporal resolution, currently available multispectral satellite imagery broadly seem to be either of high spatial but low temporal resolution or low spatial but high temporal resolution. Therefore, in this research images at two spatial resolution scales were utilised, first the high spatial resolution (30 m) Landsat Thematic Mapper/Enhanced Thematic Mapper plus (TM/ETM+), and secondly the lower spatial resolution (250 m) MODIS (Moderate Resolution Imaging Spectrometer) scale. A combination of unsupervised and supervised maximum likelihood classification of images enhanced using PCA and the Normalised Difference Vegetation Index (NDVI) was employed in the process. The accuracy of the vegetation zone mapping was judged against the established field survey-derived geology map of the park. Unlike previous remote sensing studies of KNP (e.g. Landmann 2003; Mutanga & Skidmore 2004; Mutanga et al. 2004; Verbesselt et al. 2007) this study synoptically examines the role of geology in influencing the spectral response of the vegetation in the park.

### Study area

Kruger National Park is a large (19,633 km<sup>2</sup>) narrow north-south swathe of terrestrial (savanna) habitats located on the eastern edge of South Africa (Fig. 1, inset) that was first proclaimed in 1898 and established in its current size in 1926. The northern half of the park forms part of the Great Limpopo Transfrontier Park which encompasses protected areas in the neighbouring countries of Zimbabwe and Mozambique (Weis et al. 2002; Wolmer 2003). Conservation of ecological integrity in the park involves vegetation conservation, in addition to animal conservation (Wolmer 2003). For such large conserved areas in southern Africa, discriminating and mapping the vegetation types by remote sensing is potentially useful in monitoring the state of the protected areas, thereby providing timely spatial data upon which to base conservation management strategies. The park has been stratified in a number of ways (e.g. by landscapes, by land systems, by vegetation), including the Gertenbach-Venter vegetation classification scheme (Fig. 1). This is chosen in this study because it is not too detailed for the spatial resolution of the images used but at the same time it preserves the essential features of the vegetation of the park. This classification scheme is a reworking of the older 35-zone (Gertenbach 1983), landscape based stratification of KNP (KNP GIS Section, 2008, personal communication). The characteristics of the vegetation classes in the Gertenbach-Venter scheme are related to geology, as summarised in Table 1. The area is underlain by a variety of rocks of sedimentary, igneous and metamorphic origin, with inherent fertility differences (Fig. 2). As shown in Fig. 2, generally the eastern (hilly) half of the park is made of more fertile basalt lithology, while the western half is underlain by less fertile lithology that includes granite, gneiss and arenite. The region in which KNP is located receives summer rains, from October/November to March/April.

### Methods

#### Image selection

Vegetation phenology state guided the timing of imagery utilised. Although there are variations due to edaphic and topographic factors, most woody species in the area develop spring leaf between mid-September and mid-November, and are in full mature leaf from December to May, with the peak rainfall

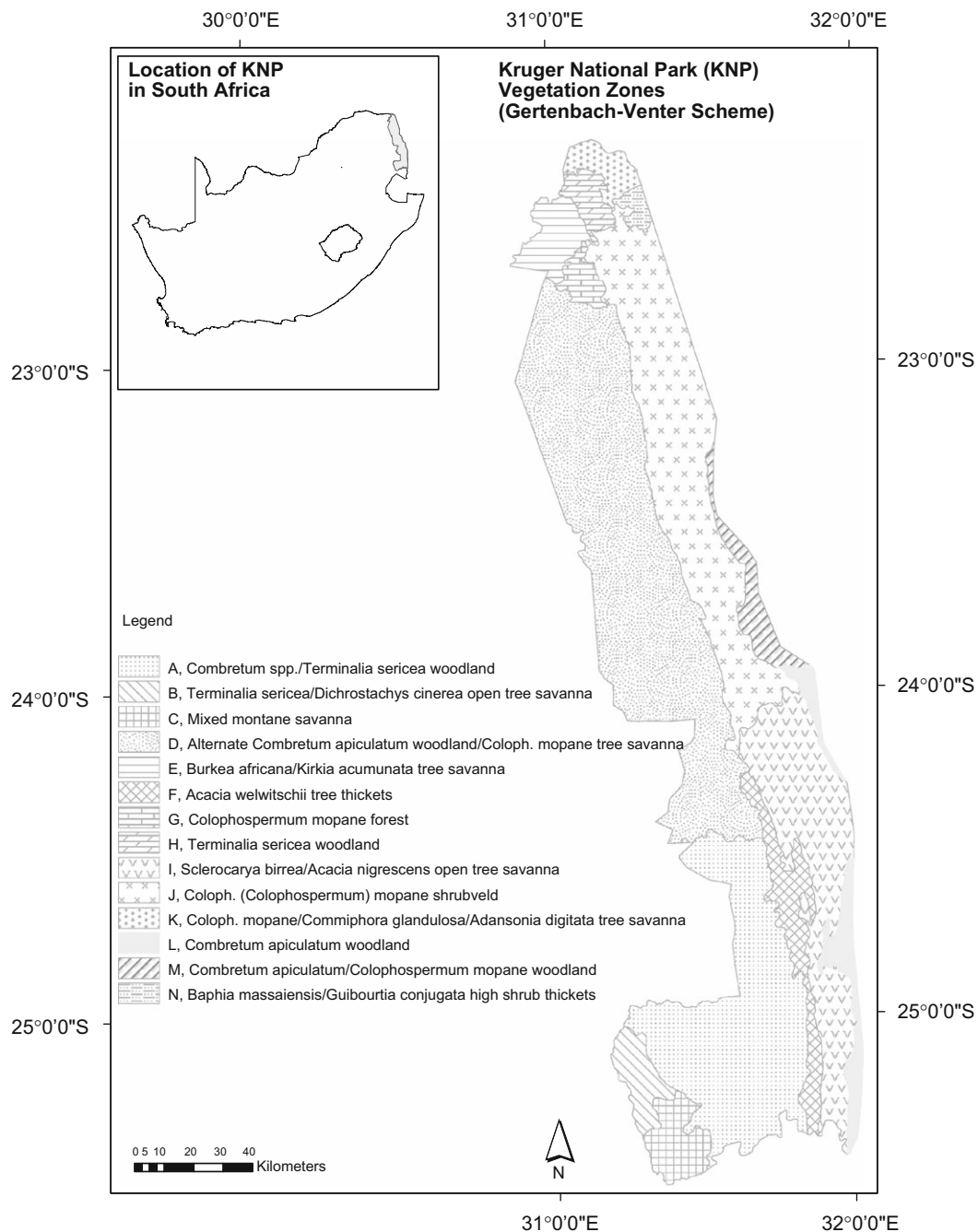


**Fig. 1.** Location and vegetation classification (based on the Gertenbach-Venter scheme) of Kruger National Park. Letters in the legend are the established abbreviated references to each of the respective full class descriptions. Legend symbols do not refer to their geologic conventional meanings. See Table 1 for description of the vegetation classes. Vegetation map source: SANParks, 2008.

period being December-January (Shackleton 1999). The phenology of herbaceous species responds to the rains. Being a protected area, human harvesting of vegetation is not a perturbation factor and apart from elephant damage of woodlands through tree felling and uprooting (Eckhardt et al. 2000) and dry season fires, the trees in the park have no major destructive agents. Rain season images were judged to be ideal for mapping the vegetation of Kruger National Park, because the vegetation is at high productivity then, limited only by geologically related edaphic factors (e.g. soil fertility), position in the landscape, wildlife grazing and occasional droughts. Dry season imagery was not ideal because the vegetation is largely leafless in winter (May-August) and also because of occasional fire damage (van Wilgen et al. 2000). Late

fires (September-November) damage emerging spring leaf in the vegetation, which has implications on spectral response of the vegetation on early rain season imagery in that such fires leave dark 'burn scars' on the vegetated landscape. In the absence of such and other major perturbations, vegetation differences as influenced by geological fertility factors can best manifest in the rain season and mapping them by remote sensing was deemed best performed in this season. However, although suitable from the vegetation phenology point of view (peak in vegetation productivity), the rain season presents difficulties in image availability for the area, due to cloud cover during the peak rainfall period (December-January).

Because of the large size of KNP (about 280 km long and nearly 70 km wide, Fig. 1), the large swath (185 x 185 km) 30 m spatial

**Table 1**  
Characteristics of Kruger National Park vegetation classes under the Gertenbach-Venter classification system.

Code	Vegetation name (dominant tree species)	Other (geology)
A	<i>Combretum</i> spp./ <i>Terminalia sericea</i> woodland	Located on granite and gneiss; sandy soil in uplands with clay soil in lowlands; woodland with sweet, mixed sparse grass.
B	<i>Terminalia sericea</i> / <i>Dichrostachys cinerea</i> open tree savanna	Located on granite and gneiss; coarse reddish deep soil in uplands and clay soil in lowlands; with mixed, sweet and tall sour grasses.
C	Mixed montane savanna	Located on granite and gneiss; very shallow stony soil in uplands with clay soil in lowlands; with mixed sour and sweet grasses.
D	Alternate <i>Combretum apiculatum</i> woodland/ <i>Cholophospermum mopane</i> tree savanna	Located on granite and gneiss with sand in the uplands and clay on lowlands; woodland with mixed and sweet grasses.
E	<i>Burkea africana</i> / <i>Kirkia acuminata</i> tree savanna	Sandy soil; woodland with sparse to moderate sweet grass.
F	<i>Acacia welwitschii</i> tree thicket	Located on ecca shales with clay soil; with short sweet grass.
G	<i>Cholophospermum mopane</i> forest	Located on ecca shales and clay soil; with sweet grass.
H	<i>Terminalia sericea</i> woodland	Sandy soil (clay in places); woodland with sparse to moderate sweet grass.
I	<i>Sclerocarya birrea</i> / <i>Acacia nigrescens</i> open tree savanna	Located on basalt and dark clay soil; with sweet grass.
J	<i>Cholophospermum mopane</i> shrubveld	Located on basalt and shallow clay soil; with sweet and mixed grasses.
K	<i>Cholophospermum mopane</i> / <i>Commiphora glandulosa</i> / <i>Andansonia digitata</i> tree savanna	Mostly on basalt; sandy soil and alluvial plains; with sparse short sweet grass.
L	<i>Combretum apiculatum</i> woodland	Located on rhyolite/basalt with shallow stony soil on upperlands and dark clay soil on the lower plains; with sweet grass.
M	<i>Combretum apiculatum</i> woodland/ <i>Cholophospermum mopane</i> woodland	Located on rhyolite/basalt with shallow stony soil on upperlands and dark clay soil on the lower plains; with sweet grass.
N	<i>Baphia massaiensis</i> / <i>Guibourtia conjugata</i> high shrub thickets	Located on basalt and shallow clay soil; with sweet and mixed grasses.

SOURCE: Summarised from Gertenbach, 1983.

resolution Landsat TM/ETM+ made images from this sensor the ideal high spatial resolution imagery for use, in comparison with those from multispectral sensors with nearly comparable (like SPOT HRV/HRVIR, 20 m) or higher (e.g. IKONOS, 4 m) spatial resolution. Four Landsat scenes are needed to cover the whole of KNP, whereas more scenes would be needed if SPOT or IKONOS images were used. Because of cloud cover the most recent summer Landsat images (November 2007–February 2008) were not usable and, consequently, older image scenes from the 2005/2006 and 2006/2007 rain seasons were utilised (Table 2). Cloud cover problems also prevented the use of same month, same year and same sensor (TM or ETM+ only) images even for these older images. However, the vegetation was phenologically similar on all the Landsat image dates because they were rain season images and, with the exception of the 16 November 2005 (WRS 169-76) image, all the images were from the same (2006/2007) rain season, differing only in terms of the cumulative amount of rains at image acquisition time. Two Landsat scenes (168-77 and 169-76) cover most of the park and the other two cover only small fractions (Fig. 3a). All the Landsat images were at level L4 (path orientated) processing level, and were subsequently projected as part of preprocessing. Although Landsat 7 experienced a Scan Line Corrector (SLC) problem in May 2003, causing large gaps at image edges (SLC-off data), a large overlap between the images from scenes 169-76 and 168-78 meant that a more central section of the ETM+ image was utilised and, therefore, no interpolation to fill data gaps was necessary for the image. A November–December 2006 MODIS image (Fig. 4a) was obtained from the ORNL DAAC (Oak Ridge National Laboratory Distributed Active Archive Center 2008) in form of a 16-day composite grid NDVI (MOD13Q1) product in GeoTIFF format, and subsequently projected to the same map projection as the Landsat images as part of image preprocessing procedures.

#### Image preprocessing

Image processing was undertaken using ERDAS Imagine 9.1 software, with additional mapping and processing undertaken using ArcGIS 9.0. It was important to utilise a common map projection for the image scenes used. Using ground control points that were visually identifiable on the images, the Landsat images

were projected to the UTM WGS84 projection (zone 36S) using nearest neighbour resampling, with subpixel root mean square error. From each reprojected image a vector shape file of the same projection outlining Kruger National Park was used for sub-setting the section of the image covering the park, resulting in the image portions (sub-scenes) in Fig. 3a. Because the sub-scenes from WRS 168-77 and 168-78 were acquired on the same day, they were joined into a mosaic prior to processing for vegetation mapping (Principal Component Analysis and image classification), whereas the sub-scenes from the northern half of KNP (WRS 168-76 and 169-76) underwent processing separately, to avoid error from modification of image data statistics introduced by joining images from different dates with differing illumination conditions. The MODIS image was also reprojected to the UTM WGS84 zone 36S map projection, using nearest neighbour resampling.

Principal Component Analysis (PCA) was used for spectral enhancement of the Landsat image subsets prior to image classification for mapping of the vegetation. In the process, all the multispectral TM/ETM+ bands were used, with the exception of the thermal bands. The resulting eigen vectors and component data variance values from the PCA are shown in Table 3a. The eigen images from principal component 1 (PC1), with more than 98% of the data variance, were selected for use in the ensuing vegetation mapping primarily because of the high spatial heterogeneity depicted, which was visually judged to depict the vegetation heterogeneity of the park best out of the six principal components (see Fig. 3b, insets). From the eigen vectors in Table 3a, this component can be interpreted as enhancing all TM bands due to the positive eigen vectors loading into it for each TM band. Automated (unsupervised) classification of each of the selected eigen image scenes using the ISODATA algorithm within ERDAS was then performed, specifying the number of output classes as 14, the number of classes in the Gertenbach-Venter classification scheme (Fig. 1). This initial image classification was subsequently used during field collection of image interpretation data.

#### Vegetation mapping and field verification

Two field visit campaigns were undertaken in the summer (rain season) period of December 2007 – February 2008, the first

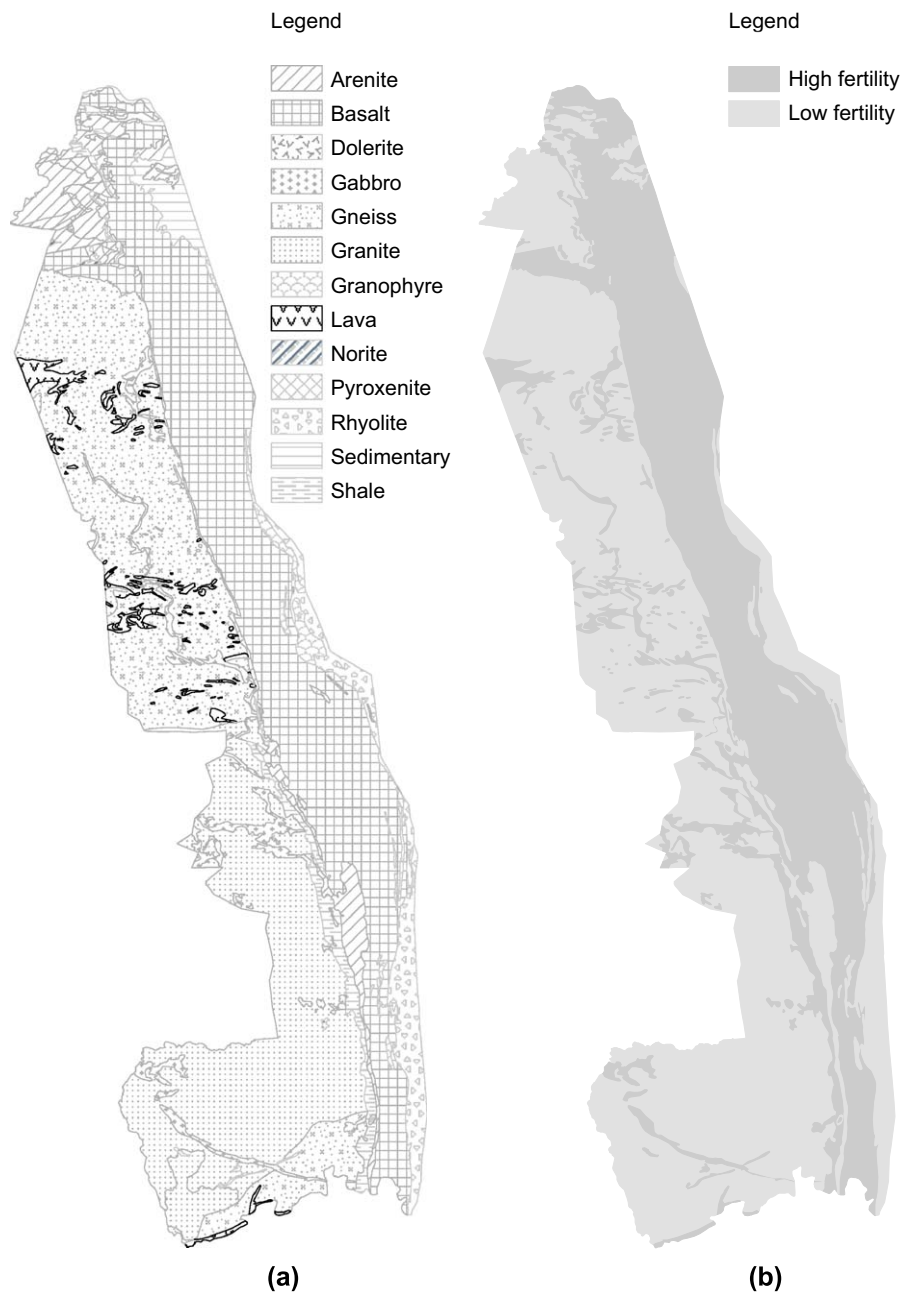


**Fig. 2.** Geology of Kruger National Park based on lithology (a) and fertility (b). Legend symbols do not refer to their geologic conventional meanings. Source: Council for Geosciences 1:1 M Geological Map of South Africa, Pretoria, South Africa.

**Table 2**

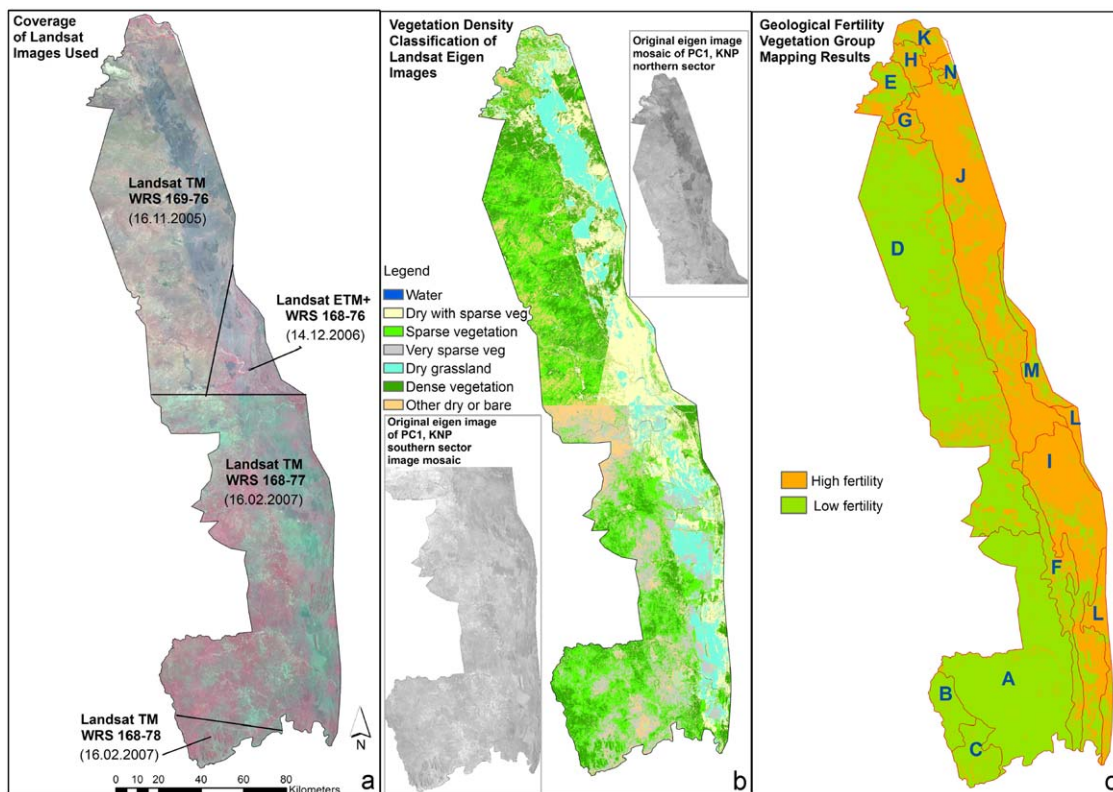
List of utilised Landsat and MODIS images covering Kruger National Park.

Image date	Sensor	Landsat WRS*	Spatial resolution
14 December 2006	Landsat 7 ETM+	168-76	30 m
16 February 2007	Landsat 5 TM	168-77	30 m
16 February 2007	Landsat 5 TM	168-78	30 m
16 November 2005	Landsat 5 TM	169-76	30 m
03 December 2006	MODIS	-	250 m

\* Scenes 169-76 and 168-77 collectively cover most of the park, while scenes 168-76 and 168-78 cover only small portions (see Fig. 3a).

(December 2007) for purposes of obtaining field condition image interpretation data, and the second (February 2008) as part of verification of accuracy of vegetation mapping. The sampling design of field locations for the image interpretation data

collection field work was established after the initial automatic (unsupervised) clustering of the image data into 14 clusters (approximating the number of classes in the Gertenbach-Venter classification scheme, Fig. 1). Thereafter, 14 locations representing the respective initial clusters and in proximity to the park's public access roads were visited, mainly in the southern section of KNP. During the visits vegetation description information (vegetation density and Gertenbach-Venter class) was recorded, photographs taken for future reference and GPS readings of the locations taken. Accessibility is a constraint to field sampling in mapping biodiversity of such inaccessible wilderness areas using remote sensing (e.g. Buchanan et al. 2008; Fuller et al. 1998), often resulting in a statistically less representative sampling design. In this work the ideal field sampling design would have been a stratified random sampling scheme (elaborated by McCoy 2005), with the number of sample points per cluster (stratum)



**Fig. 3.** Landsat TM/ETM+ image sub-scenes (RGB 432) of Kruger National Park depicting images used in the study (a), result of image processing showing vegetation density image classification (b), and extent of correlation between image derived vegetation analysis and the Gertenbach-Venter vegetation classes of KNP (red lines) in comparison with geologic fertility strata (c). The image in (b) is from classification of the inset eigen images of principal component 1 of the respective sub-scenes in (a) whose eigen vectors are shown in Table 3a. The capital letters in (c) refer to the Gertenbach-Venter vegetation classes in Fig. 1 and Table 1.

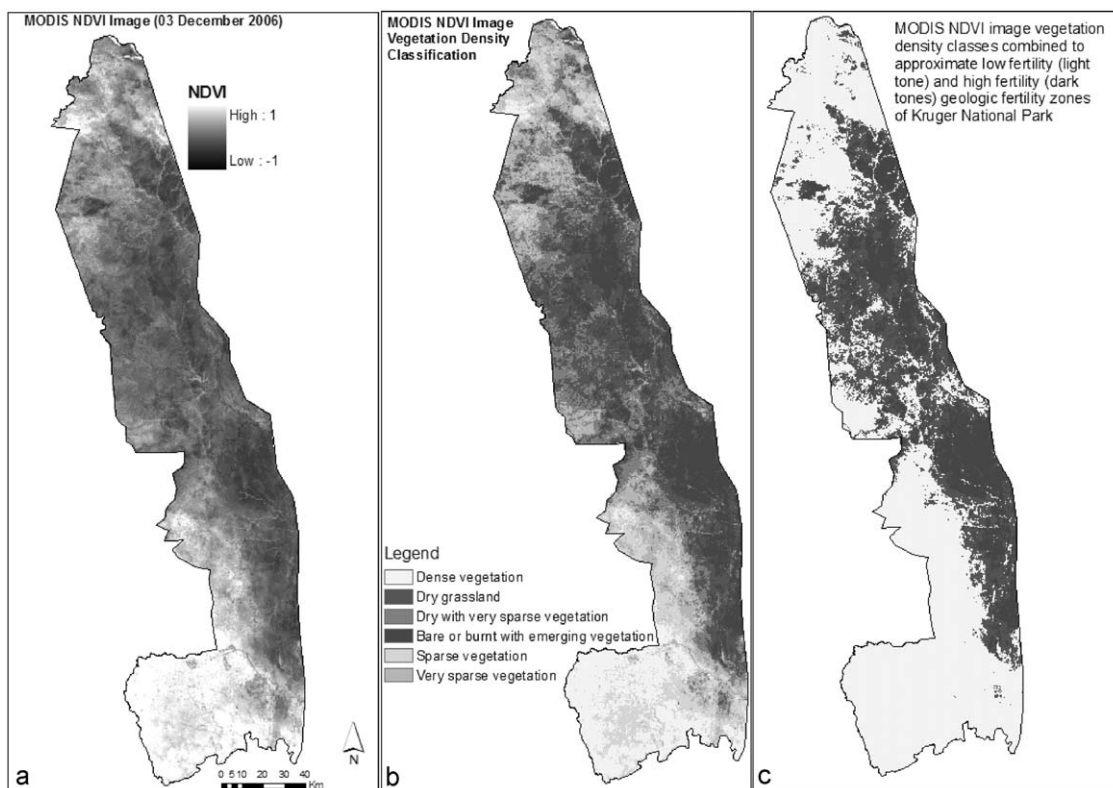


**Fig. 4.** MODIS 3 December 2006 NDVI image of Kruger National Park showing variation in greenness of the park's vegetation (a), the image classified into vegetation density classes (b) and the relationship between the vegetation density classes and the park's geologic fertility zones (c) (compare with Fig. 2).

**Table 3**

Eigen vectors, data variance values and spectral signatures from principal component analysis of the Landsat image sub-scenes utilised for the vegetation mapping of Kruger National Park.

(a) Eigen vectors and data variance values for principal component 1 (PC1)			
	PC1 from sub-scene 169-76, 16 November 2005	PC1 from sub-scene 168-76, 14 December 2006	PC1 from mosaic of sub-scenes 168-77 and 168-78, 16 February 2007
TM1	0.39964	0.41793	0.46343
TM2	0.19428	0.20084	0.21540
TM3	0.27233	0.26416	0.23812
TM4	0.31803	0.33199	0.45376
TM5	0.70207	0.69219	0.63118
TM7	0.36652	0.35479	0.27900
% variance	99.053	99.366	98.159
(b) Class spectral signature statistics from PC1 eigen image			
Class name	Class mean in PC1	St. deviation (s)	
Dense vegetation	141.4	6.79	
Sparse vegetation	153.4	4.70	
Very sparse vegetation	166.0	5.28	
Dry with very sparse vegetation	149.6	3.67	
Dry grassland	159.9	6.14	
Other dry or bare land	187.7	12.38	
Water	65.4	14.16	

dependent on its size. A less subjective vegetation density quantification method, for example using densiometer crown cover estimates, would also have improved the field site categorisation of vegetation density. The 14 sites served as training areas for subsequent image interpretation for classification purposes. Descriptive data from a further 23 accessible sites representing these clusters were recorded in February 2009 for purposes of improving the representation from training areas, bringing the total number of training sites to 37. Because the goal of field work after initial clustering in unsupervised classification is to identify the information class represented by each cluster (McCoy 2005), this additional descriptive work was useful in further confirming the vegetation condition represented by the clusters. Such qualitative field vegetation descriptions have commonly been utilised and shown to be adequate for purposes of image classification (e.g. Brandt & Townsend 2006; Cingolani et al. 2004; Ravan et al. 1995; Sà et al. 2003) and are sometimes the only practical option when there are time and hazard constraints, compared to quantitative descriptions on field plots (Treitz et al. 1992). Treitz et al. (1992) established that a qualitative approach to field-plot description produces a more statistically accurate digital classification of remotely sensed data than does the detailed (TWINSPAN) quantitative ground information. In this work we faced season-related time constraints and, to some extent, accessibility and the hazard of wildlife, necessitating the use of qualitative descriptive data, which was taken from training sites extending approximately 100x100 m and selected on the basis of vegetation homogeneity. Therefore, the field data were collected from homogenous training sites encompassing at least three 30 m Landsat pixels.

The initial field work revealed that the initial 14 clusters resulting from unsupervised classification did not match the 14 Gertenbach-Venter vegetation classes (Table 1) and could not be named consistently. However, the field work revealed that the initial 14 clusters could be regrouped into six cover classes representing variation in vegetation density and phenology stage, namely dense vegetation, sparse vegetation, very sparse vegetation, dry with very sparse vegetation (i.e. dry areas with very

scattered trees), dry grassland, and other dry (or bare) land (Table 3b). Because KNP is wholly in the savanna biome, we utilised the following definition of savanna in assigning class vegetation density thresholds: "woodland (savanna) is typically vegetation with a grass-dominated herbaceous layer and scattered low to tall trees; it includes the closed woodland and open woodland of Edwards (1983) with a tree cover less than 75% and generally greater than 1%" (Mucina & Rutherford 2006). Implicit in this definition is the inherent scattered tree nature of savannas. Therefore, based on the definition and site specific observations we devised a scheme in which we categorised woody vegetation cover  $\geq 60\%$  as dense vegetation,  $50 - < 60\%$  as sparse vegetation, and  $< 50\%$  as very sparse vegetation, for purposes of field site tree cover differentiation. Subsequently, a supervised maximum likelihood classification of each of the principal component Landsat image subsets was performed using the six vegetation density classes (class names based on field visit training sites) plus a water class, and the resulting thematic layers were then combined into a mosaic covering the whole of KNP. The MODIS NDVI product image obtained was also processed so as to produce this six class vegetation density gradient. A number of studies (e.g. Kogan et al. 2003; Kumar et al. 2007) have shown the NDVI and related vegetation indices to be successful in depicting vegetation density (Kerr & Ostrovsky 2003). The NDVI thresholds indicative of the different density classes vary depending on the vegetation type. On the MODIS NDVI image, the vegetation in the vicinity of our training sites exhibited NDVI values  $> 0.40$  for dense vegetation,  $0.30 - < 0.40$  for sparse vegetation, and  $< 0.30$  for very sparse vegetation. Because the training sites were selected on the basis of homogeneity and were large enough for spatial inference to the 250 m MODIS pixel, these NDVI thresholds were utilised in the classification of the MODIS NDVI image into the vegetation density gradient classes. Though working at the 500 m pixel scale, Chongo et al. (2007) report comparable indicative MODIS NDVI November mean values of 0.35-0.65 for unburned areas in KNP from 2001, 2002 and 2003 images. Water (in rivers, artificial water provision holes) was largely indistinguishable at the 250 m pixel scale on the MODIS image and, therefore, the MODIS classification excluded the water class.

Accuracy assessment for the resulting vegetation density image classification was undertaken using a stratified random sample of 256 pixels for the Landsat classification only, primarily because the 250 m pixel representation of the MODIS image made field location of sample pixels more difficult. Since the location of the sample pixels was completely random in the park, they could not easily be visited because the majority of them were far from the park's public access roads and could only be reached on foot, a very arduous and time consuming process (also potentially dangerous due to possible animal attacks). Twenty seven (27) of the randomly generated sample locations were in proximity ( $< 1$  km) of the park's public access roads and were, therefore, visited in February 2008 as part of classification accuracy assessment. For the remaining 229 random sites, the approach by Buchanan et al. (2008) involving use of the high spatial resolution (0.61-2.40 m) QuickBird® imagery on GoogleEarth® as reference data was adopted for this work. Because the GoogleEarth images are georeferenced in latitude and longitude (degrees, minutes, seconds) we converted the coordinates of the remaining 229 randomly generated accuracy assessment points to degrees, minutes and seconds, and navigated to each site to verify correctness of the respective class assignments. Although the ideal would have been to use field visits (or aerial photographs) as reference data, these images were utilised as substitute due to accessibility problems and have been found to be useful as reference data for remote wilderness areas where accessibility is a problem (Buchanan et al. 2008). Because of the high spatial

resolution of the GoogleEarth imagery (acquired during the rain season), individual trees were discernable, enabling the estimation of tree cover percentage in relation to the image classification classes used, and a comparison with the Landsat image using identifiable features (trees, paths) for scale. The resulting overall classification accuracy was 89.1% (KHAT = 87.6%; Table 4).

The resulting six class classification of the Landsat and MODIS images depicting a vegetation density gradient was then evaluated to assess the extent to which the Gertenbach-Venter vegetation classes were reproduced. A process of classification class merger was then performed in order to match the classes with the geologic fertility zones (high versus low, Fig. 2) of the park. The low fertility zone could be approximated by merging the dense vegetation, sparse vegetation, and very sparse vegetation classes, with the remainder of the classes largely delineating the high fertility zone (relationship between fertility and tree community structure explained in Discussion section). Dense vegetation, sparse vegetation, and very sparse vegetation classes collectively indicate tree cover and, therefore, woodland (savanna;

see definition above), hence their merger into one class. Accuracy assessment of this final geological fertility vegetation map was then performed. The 256 random points generated for accuracy assessment of the Landsat image classification were retained and utilised in statistical assessment of the accuracy of the Landsat and MODIS-derived final classification maps approximating the two geological fertility strata of the park.

## Results

The results of the vegetation density classification using Landsat imagery are shown in Fig. 3b. The vegetation mapping scheme was successful in reproducing some of the riparian vegetation, but the 14 Gertenbach-Venter vegetation classes (Fig. 1) are largely indistinguishable (Fig. 3b). However, at the less detailed stratification level of the two geological fertility zones (Fig. 2), the Landsat vegetation mapping scheme does approximate the high and low fertility zones of the park (compare

**Table 4**  
Landsat image classification accuracy assessment.

(a) Classification error matrix		Reference data							Total	User's accuracy (%)
Classification data		Class 1	Class 2	Class 3	Class 4	Class 5	Class 6	Class 7		
Class 1 (Dense vegetation)		47	3						50	94.0
Class 2 (Sparse vegetation)			45	2					47	95.7
Class 3 (Very sparse vegetation)			5	34	1				40	85.0
Class 4 (Dry+very sparse vegetation)				5	28	5			38	73.7
Class 5 (Dry grass)				1	2	52	1		56	92.9
Class 6 (Other dry or bare land)					2	1	19		22	86.4
Class 7 (Water)								3	3	100
Total		47	53	42	33	58	20	3	256	
Producer's accuracy (%)		100	84.9	81.0	84.8	89.7	95.0	100		
Overall accuracy = 89.1%										
KHAT (overall) = 87.6%										
(b) Relationship between image classification and field description for 27 accessible accuracy assessment sample sites										
Site	GPS coordinates (UTM, meters)	Field description	Image classification class (* = incorrect classification)					Gertenbach-Venter class (Fig. 1)		
1.	358124, 7233722	Scattered trees and dry grass	Sparse vegetation					D		
2.	357394, 7231952	Thick acacia bush	Dense vegetation					D		
3.	357733, 7229751	Scattered trees, shrubs and grass	Sparse vegetation					D		
4.	355103, 7227678	Scattered trees, shrubs and grass	Sparse vegetation					D		
5.	354641, 7227490	Shrubs, grass, herbs; 95% open	Bare, dry					A		
6.	353159, 7220696	Very open (about 90% open), few trees/ grass	Sparse vegetation *					A		
7.	359536, 7220696	Water hole, bare parts, woodlands	Dry with sparse vegetation					A		
8.	346965, 7236433	Sabie river riparian vegetation	Sparse vegetation					H		
9.	333109, 7236281	Scattered trees, <i>hyparrhenia</i> grasses	Bare, dry *					D		
10.	326680, 7234168	Sparsely vegetated, lots of grass	Sparse vegetation					E		
11.	326160, 7234540	Densely vegetated	Dense vegetation					E		
12.	324704, 7226786	Sparsely vegetated, dry grass	Sparse vegetation					B		
13.	335192, 7210629	<i>Kopjie</i> (rock hill), short shrubs surrounding	Dense vegetation *					C		
14.	356817, 7195676	Dense vegetation	Sparse vegetation *					A		
15.	369999, 7279340	Dense vegetation, scattered shrubs, dry grass	Sparse vegetation *					A		
16.	375192, 7201869	Tree-grass mixture, nearly 50% tree cover	Dry, very sparse vegetation					A		
17.	388046, 7215956	Dense vegetation with dry grass	Dense vegetation					D		
18.	362835, 7238450	Acacia thickets with bare ground	Sparse vegetation					G		
19.	368696, 7253325	Sparse vegetation	Sparse vegetation					A		
20.	379000, 7267770	Sparse dry trees and dry grasses	Dry, very sparse vegetation					G		
21.	377631, 7277329	Sparse vegetation	Sparse vegetation					G		
22.	377129, 7297282	Grassland area with sparse trees	Sparse vegetation					F		
23.	373989, 7307625	Dry grass	Dry grassland					F		
24.	366871, 7335370	Woodland, nearly 50% tree cover	Sparse vegetation					J		
25.	364056, 7343534	Predominantly mopane trees, 60% cover	Dense vegetation					L		
26.	353298, 7360482	Predominantly short mopane shrubs	Dense vegetation					L		
27.	341321, 7354448	Short mopane shrubs with grass	Dense vegetation					D		

**Table 5**

Comparison between the geological fertility map of Kruger National Park and the image processing classification of vegetation into geological fertility zones based on a random sample of locations.

	Geology map	Landsat classification correctly classified points	MODIS classification correctly classified points
High fertility	104 sample points	80 (= 77%)	68 (= 65%)
Low fertility	152 sample points	130 (= 86%)	103 (= 68%)
Totals	256 sample points	210 (= 82%)	171 (= 67%)

Figs. 3c and 2b). The Landsat vegetation mapping correctly assigned 82% of the random points used in accuracy assessment into their respective high and low fertility zones of the park (Table 5), with an overall KHAT ( $K^{\wedge}$ ) statistic of 0.75, indicating that it avoided 75% of the errors that a completely random classification would generate. The spatially more homogenous low fertility zone was better mapped by the Landsat mapping, with 86% accuracy compared to 77% for the spatially more fragmented high fertility zone.

The results of vegetation mapping using the rain season MODIS image are shown in Figs. 4b and c. Like the Landsat imagery, vegetation mapping using the MODIS image was unable to separate the 14 Gertenbach-Venter vegetation classes but was able to distinguish between the high fertility and low fertility zones of KNP, with 67% overall accuracy (Table 5). However, unlike the mapping results from the Landsat imagery, MODIS mapping was only marginally more accurate in correctly assigning the random points to the spatially more homogenous low fertility zone (68% of the random pixels) compared to the spatially more fragmented high fertility zone (65% of the random pixels), which can be attributed to the lower spatial resolution of MODIS in that on the lower (250 m) MODIS spatial resolution, some vegetation on linear and isolated small patches of the high and low fertility zones (see Fig. 2b) could not be mapped as distinct from that in the surrounding fertility zone, compared to the case with the higher (30 m) Landsat TM/ETM+ spatial resolution. The MODIS vegetation mapping with an overall accuracy of 67% avoided only 57% of the errors that a completely random classification would generate ( $K^{\wedge} = 0.57$ ). However, the accuracy of the MODIS mapping was not significantly different from that of the Landsat mapping ( $\chi^2 = 0.1108$ ,  $P > 0.05$ ), which can be attributed to the fact that linear and isolated small patches of the high and low fertility zones are only a small fraction of the respective contiguous and larger zones in their category (Fig. 2b).

Therefore, vegetation mapping using Landsat TM and MODIS imagery of the summer (rain season) period when vegetation is at high productivity showed that the vegetation of KNP is not separable on the basis of the 14 class Gertenbach-Venter classification scheme (Fig. 1) that uses dominant tree species for class definition (Table 1). However, the 14 classes are also related to the underlying geology of the park (compare Figs. 1 and 2) and from the results of this work the vegetation of KNP can reasonably be delineated (accuracies of 67–82%) using Landsat and MODIS imagery on the basis of geologic fertility as shown in Figs. 3 and 4, using image processing techniques that differentiate vegetation density and vigour. This implies that the underlying geology of KNP has a strong influence on vegetation community structure and density and, thereby, intensity of reflectance in the visible–mid infrared spectral regions, which can be detected by moderately to high spatial resolution sensors detecting reflected electromagnetic radiation with broad spectral resolution in the visible, near and mid infrared spectral regions.

## Discussion

The low fertility and high fertility substrates of KNP, through edaphic and landscape characteristics, influence the vegetation

structure and density to a sufficiently strong extent that the spectral reflectance characteristics between the two zones are distinguishable on multispectral remotely sensed imagery, as shown in this study. The soils of the high fertility zone, derived from basic rocks (including basalts; Fig. 2), are fine textured and support mainly multiple-stemmed shrubs, whereas the low fertility zone's soils (parent lithology being granitic gneiss, etc) are coarse-textured, supporting mixed savanna woodlands (Fraser et al. 1987). These are the contrasting tree community structures that are distinguishable on multispectral images. The ability to map the high fertility and low fertility vegetation zones of KNP from remotely sensed imagery is significant for monitoring the park's vegetation, because a number of ecological analyses of relevance to conservation management of the park have used the contrast between the two, or the influence of either or both. In a study of long-term change in woody vegetation cover (trees and shrubs combined) in the park, Eckhardt et al. (2000) established that woody cover increased by 12% on granite (low fertility) substrates but decreased by 64% in basalt (high fertility) areas between 1940 and 1998, the decline in large trees was attributed to the interaction between regular, frequent fires and utilisation by elephants. The severe changes in tree density on the basaltic plains in KNP are a cause for concern (Brits et al. 2002). The low-versus high-fertility zone contrast also has implications for fire frequency in the park. According to van Wilgen et al. (2000), fires tend to be more frequent in the southwest (low fertility) section of the park compared to the high fertility southeast partly because the low nutrient status of the soils in the southwest section results in relatively low grazing pressure, resulting in grass fuels accumulating during the rain season, in contrast with the high fertility (basalt substrate) southeast section where grasses are more palatable and tend to be heavily grazed.

The low separability of the vegetation species based Gertenbach-Venter vegetation zones of KNP (Table 1) on broad band multispectral imagery such as Landsat TM and MODIS is attributable partly to the spectral resolution of the Landsat Thematic Mapper (TM) and the MODIS sensor, collectively with broad bands in the visible, near and mid infrared spectral regions that are unable to differentiate tree species spectral reflectance, and partly to the overlaps in species composition of the vegetation zones. Higher spectral resolution hyperspectral imagery processed using sub-pixel classification techniques potentially could differentiate the trees species spectrally, but would probably still not reproduce the vegetation zones because of the species composition overlaps. For example, vegetation zones D, G, J, K, and M (Table 1) have one common tree species, *Cholophospermum mopane*, while zones A, D, L and M all have *Combretum* species in common (with zone C being 'mixed'). Therefore, out of the 14 zones, 7 zones (A, C, D, G, J, K, L, and M) or 50% of the vegetation types are of mixed species composition. Although the tree species which these vegetation zones have in common occur in different abundances and in combination with other species, the generalised spectral signature on the broad spectral ranges of multi-spectral imagery results in low separability. This low spectral separability due to common species in the vegetation zones of KNP explains why the vegetation was only broadly distinguishable

on the basis of geologic fertility (Figs. 3 and 4). For broadly defined habitat types, the results from this study are comparable with results from similar broad habitat type mapping studies using remote sensing in similar savanna environments (e.g. Ringrose et al. 2003).

Using the 85% minimum accuracy threshold for Level I mapping by the 2000 South African National Land Cover (NLC2000) project (Fairbanks et al. 2000), the Landsat image classification accuracy of 89.1% makes the methodology employed in distinguishing the high and low geological fertility zones of KNP in this study sufficiently reliable, making the results indicative of the potential of monitoring the habitats of the park using remote sensing on the basis of this broad geological fertility stratification. The Landsat image dates utilised, though from different months (November, December, February; Table 2), were mostly from the same (2006/2007) rain season, differing only in terms of the cumulative amount of rainfall. The November to early December period is towards the start of the rain season, hence the presence of dry grass and burn scars (burn scars were incorporated into the dry grassland class) in the image scenes (scene 169-76 in Fig. 3a) and because the rains were rather low and ended early in the 2006/2007 season, the February 2007 image acquisition period of two of the Landsat images used was equivalent to the November-December 2006 period in that by then some of the grass had dried out. The MODIS image was from the same period of the 2006/2007 rain season as most of the Landsat images, making the results of the vegetation mapping using the MODIS image comparable. There also was a burn scar on the MODIS scene (compare Figs. 4a and 3a).

Sensor differences for the Landsat images utilised have little effect on the results because the same multispectral bands on Landsat TM and ETM+ images (visible, near- and mid-infrared bands) were used, and with respect to these bands (apart from calibration) there have been no changes in spatial or spectral resolution between the TM and ETM+ sensors (Lillesand et al. 2004) which were the two sensor characteristics that were central to the analysis in this study. Differential atmospheric effects on the different Landsat image dates had little effect on the accuracy of the results because images from different dates were processed separately. In image classification involving a multirate Landsat TM image data set, as long as the training data for the classification are separately derived from the respective images being classified, as was the case in this work, atmospheric correction is unnecessary (Song et al. 2001) and, therefore, differential atmospheric effects (scattering and absorption) have little effect on the analysis. The eigen images selected for further use in vegetation mapping from the Landsat images (Table 3; Fig. 3b) were appropriate. PCA is (inherently) scene dependent (Eklundh & Singh 1993), and different factor loadings for the same variables (TM bands in this case) can result from different scenes, which need to be interpreted as appropriate to determine usefulness for the particular analysis (Call et al. 2003; Conese et al. 1988, including minority pixels of interest (Cheng et al. 2006)). Woody vegetation cover in the sections depicted by the two principal component images is unlikely to have changed between the two successive rain season dates of the images used in deriving them.

The large north-south spatial dimension of KNP implies that using the high spatial resolution low swath width images from sensors on satellites such as SPOT, IKONOS, OrbView, QuickBird, etc, though likely to result in greater spatial detail of vegetation in large protected areas like KNP, would present even more synoptic coverage and date difference difficulties than those encountered in this study (illustrated in Fig. 3a). There is scope for the combined use of such high spatial resolution imagery as supplement to large swath width, high temporal frequency, low

spatial resolution imagery such MODIS in habitat monitoring for large protected savanna areas in a two scale analysis framework; using the low spatial resolution imagery as indicator of sections of habitat to study at greater detail. In Kruger National Park, MODIS imagery is already routinely utilised to monitor fires, using two images a day (KNP GIS Section, 2008, personal communication), which could be adopted by savanna protected area authorities in the rest of Africa when technical facilities are available (e.g. there are MODIS imagery receiving stations in South Africa and none in much of the rest of Africa). As shown by this study broad scale vegetation zone mapping for large savanna habitats can be accomplished using common image processing algorithms backed by ecological knowledge of the habitats represented, through careful selection of sensor, image processing method and timing of imaging acquisition period. The resulting habitat mapping is potentially useful in the management of the protected areas in enabling rapid update of habitat state and quantifying the spatial changes for purposes of possible management intervention as deemed necessary. There is, therefore, potential for adoption of such routine habitat mapping and monitoring using remote sensing and GIS in the conservation of large protected savanna areas.

### Acknowledgements

This research was facilitated by a postgraduate scholarship grant to the University of Venda under the German Academic Exchange Services (DAAD) in-country scholarship scheme, and by a Council for Scientific and Industrial Research (CSIR) Scientific Cooperation project grant for collaboration between the CSIR's Ecosystems Earth Observation Research Group and the School of Environmental Sciences of the University of Venda. The authors are grateful for the assistance received from staff in the Scientific Services division of Kruger National Park at Skukuza, in particular the GIS section for providing spatial data that guided the vegetation mapping and field work, as well as the game guards whose escorting presence during field work provided a reassuring sense of protection from animal attacks.

### References

- Bock, M., Panteleimon, X., Mitchley, J., Rossner, G., & Wissen, M. (2005). Object-oriented methods for habitat mapping at multiple scales – Case studies from Northern Germany and Wye Downs, UK. *Journal for Nature Conservation*, 13, 75–89.
- Brandt, J. S., & Townsend, P. A. (2006). Land use–land cover conversion, regeneration and degradation in the high elevation Bolivian Andes. *Landscape Ecology*, 21, 607–623.
- Brits, J., van Rooyen, M. W., & van Rooyen, N. (2002). Ecological impact of large herbivores on the woody vegetation at selected watering points on the eastern basaltic soils in the Kruger National Park. *African Journal of Ecology*, 40, 53–60.
- Buchanan, G. M., Butchart, S. H.M., Dutton, G., Pilgrim, J. D., Steininger, M. K. Bishop, K. D., et al. (2008). Using remote sensing to inform conservation status assessment: estimates of recent deforestation rates on New Britain and the impacts upon endemic birds. *Biological Conservation*, 141, 56–66.
- Call, K. A., Hardy, J. T., & Wallin, D. O. (2003). Coral reef habitat discrimination using multivariate spectral analysis and satellite remote sensing. *International Journal of Remote Sensing*, 24, 2627–2639.
- Cheng, Q., Linhai, J., & Panahi, A. (2006). Principal component analysis with optimum order sample correlation coefficient for image enhancement. *International Journal of Remote Sensing*, 27, 3387–3401.
- Chongo, D., Nagasawa, R., Ahmed, A. O.C., & Perveen, F. (2007). Fire monitoring in savanna ecosystems using MODIS data: a case study of Kruger National Park, South Africa. *Landscape and Ecological Engineering*, 3, 79–88.
- Cingolani, A. M., Renison, D., Zak, M. R., & Cabido, M. R. (2004). Mapping vegetation in a heterogeneous mountain rangeland using landsat data: an alternative method to define and classify land-cover units. *Remote Sensing of Environment*, 92, 84–97.
- Conese, C., Maracchi, G., & Maselli, F. (1993). Improvement in maximum likelihood classification performance on highly rugged terrain using principal components analysis. *International Journal of Remote Sensing*, 14, 1371–1382.

- Conese, C., Maracchi, G., Miglietta, F., Maselli, F., & Sacco, V. M. (1988). Forest classification by principal component analysis. *International Journal of Remote Sensing*, 9, 1597–1612.
- Congalton, R. G., Birch, K., Jones, R., & Schriever, J. (2002). Evaluating remotely sensed techniques for mapping riparian vegetation. *Computers and Electronics in Agriculture*, 37, 113–126.
- Eckhardt, C. H., Wilgen, W. B., & Biggs, C. H. (2000). Trends in woody vegetation cover in the Kruger National Park, South Africa, between 1940 and 1998. *African Journal of Ecology*, 38, 108–115.
- Edwards, D. (1983). A broad-scale structural classification of vegetation for practical purposes. *Bothalia*, 14, 705–712.
- Eklundh, L., & Singh, A. (1993). A comparative analysis of standardised and unstandardised principal components analysis in remote sensing. *International Journal of Remote Sensing*, 14, 1359–1370.
- Fairbanks, D. H.K., Thompson, M. W., Vink, D. E., Newby, T. S., van den Burg, H. M., & Everard, D. A. (2000). The South African land-cover characteristics database: A synopsis of the landscape. *South African Journal of Science*, 96, 69–82.
- Fraser, S. W., van Rooyen, T. H., & Verster, E. (1987). Soil–plant relationships in the central Kruger National Park. *Koedoe*, 30, 19–34.
- Fuller, R. M., Groom, G. B., Mugisha, S., Ipulet, P., Pomeroy, D., & Katende, A. (1998). The integration of field survey and remote sensing for biodiversity assessment: A case study in the tropical forests and wetlands of Sango Bay, Uganda. *Biological Conservation*, 86, 379–391.
- Gertenbach, W. P.D. (1983). Landscapes of the Kruger National Park. *Koedoe*, 26, 9–121.
- Kerr, J. T., & Ostrovsky, M. (2003). From space to species: Ecological applications for remote sensing. *Trends in Ecology and Evolution*, 18, 299–305.
- Kogan, F., Gitelson, A., Zakarin, E., Spivak, L., & Leved, L. (2003). AVHRR-based spectral vegetation index for quantitative assessment of vegetation state and productivity: Calibration and validation. *Photogrammetric Engineering and Remote Sensing*, 69, 899–906.
- Kumar, A., Uniyal, S. K., & Lal, B. (2007). Stratification of forest density and its validation by NDVI analysis in a part of western Himalaya, India using remote sensing and GIS techniques. *International Journal of Remote Sensing*, 28, 2485–2495.
- Landmann, T. (2003). Characterizing sub-pixel Landsat ETM+ fire severity on experimental fires in the Kruger National Park, South Africa. *South African Journal of Science*, 99, 357–360.
- Lee, J. B., Woodyatt, A. S., & Berman, M. (1990). Enhancement of high spectral resolution remote sensing data by a noise-adjusted principal components transform. *IEEE Transactions on Geoscience and Remote Sensing*, 28, 295–304.
- Lillesand, T. M., Kiefer, R. W., & Chipman, J. W. (2004). *Remote Sensing and Image Interpretation*. New York: Wiley.
- Lucas, R., Rowlands, A., Brown, A., Keyworth, S., & Bunting, S. (2007). Rule-based classification of multi-temporal satellite imagery for habitat and agricultural land cover mapping. *ISPRS Journal of Photogrammetry & Remote Sensing*, 62, 165–185.
- McCarthy, J., Gumbrecht, T., & McCarthy, T. S. (2005). Ecoregion classification in the Okavango Delta, Botswana from multitemporal remote sensing. *International Journal of Remote Sensing*, 26, 4339–4357.
- McCoy, R. M. (2005). *Field methods in remote sensing*. New York: The Guilford Press.
- Mehner, H., Cutler, M., Fairbairn, D., & Thompson, G. (2004). Remote sensing of upland vegetation: the potential of high spatial resolution satellite sensors. *Global Ecology and Biogeography*, 13, 359–369.
- Mucina, L., & Rutherford, M. C. (Eds.). (2006). *The vegetation of South Africa, Lesotho and Swaziland. Strelitzia 19*. Pretoria, South Africa: South African National Biodiversity Institute (SANBI).
- Mutanga, O., & Skidmore, A. K. (2004). Integrating imaging spectroscopy and neural networks to map grass quality in the Kruger National Park, South Africa. *Remote Sensing of Environment*, 90, 104–115.
- Mutanga, O., Skidmore, A. K., & Prins, H. H.T. (2004). Predicting in situ pasture quality in the Kruger National Park, South Africa, using continuum-removed absorption features. *Remote Sensing of Environment*, 89, 393–408.
- Nagendra, H. (2001). Using remote sensing to assess biodiversity. *International Journal of Remote Sensing*, 22, 1400–2377.
- Oak Ridge National Laboratory Distributed Active Archive Center (ORNL DAAC) (2008). *MODIS subsetted land products, Collection 5. Available on-line from ORNL DAAC, Oak Ridge, Tennessee, USA*. <<http://daac.ornl.gov/MODIS/modis.html>>; accessed 15.10.2008.
- Ringrose, S., Matheson, W., & Boyle, T. (1988). Differentiation of ecological zones in the Okavango Delta, Botswana, by classification and contextual analyses of Landsat MSS data. *Photogrammetric Engineering and Remote Sensing*, 54, 601–608.
- Ringrose, S., Vanderpost, C., & Matheson, W. (2003). Mapping ecological conditions in the Okavango delta, Botswana using fine and coarse resolution systems including simulated SPOT vegetation imagery. *International Journal of Remote Sensing*, 24, 1029–1052.
- Ravan, S. A., Roy, P. S., & Sharma, C. M. (1995). Space remote sensing for spatial vegetation characterization. *Journal of Biosciences*, 20, 427–438.
- Sà, A. C.L., Pereira, J. M.C., Vasconcelos, M. J.P., Silva, J. M.N., Ribeiro, N., & Awase, A. (2003). Assessing the feasibility of sub-pixel burned area mapping in miombo woodlands of northern Mozambique using MODIS imagery. *International Journal of Remote Sensing*, 24, 1783–1796.
- Sader, S. A., Powell, G. V.N., & Rappole, J. H. (1991). Migratory bird habitat monitoring through remote sensing. *International Journal of Remote Sensing*, 12, 363–372.
- SANParks (South African National Parks) Kruger National Park – GIS (2008). URL: <<http://www.sanparks.org/parks/kruger/conservation/scientific/gis/>>.
- Shackleton, C. M. (1999). Rainfall and topo-edaphic influences on woody community phenology in South African savannas. *Global Ecology and Biogeography*, 8, 125–136.
- Song, C., Woodcock, C. E., Seto, K. C., Lenney, M. P., & Macomber, S. A. (2001). Classification and change detection using Landsat TM data: when and how to correct atmospheric effects?. *Remote Sensing of Environment*, 75, 230–244.
- Treitz, P. M., Howarth, P. J., Suffling, R. C., & Smith, P. (1992). Application of detailed ground information to vegetation mapping with high spatial resolution digital imagery. *Remote Sensing of Environment*, 42, 65–82.
- van Wilgen, B. W., Biggs, H. C., O'Regan, S. P., & Mare, N. (2000). A fire history of the savanna ecosystems in the Kruger National Park, South Africa, between 1941 and 1996. *South African Journal of Science*, 96, 167–178.
- Verbesselt, J., Somers, B., Lhermitte, S., Jonckheere, I., van Aardt, J., & Coppin, P. (2007). Monitoring herbaceous fuel moisture content with SPOT VEGETATION time-series for fire risk prediction in savanna ecosystems. *Remote Sensing of Environment*, 108, 357–368.
- Verlinden, A., & Masogo, R. (1997). Satellite remote sensing of habitat suitability for ungulates and ostrich in the Kalahari of Botswana. *Journal of Arid Environments*, 35, 563–574.
- Weiers, S., Bock, M., Wissen, M., & Rossner, G. (2004). Mapping and indicator approaches for the assessment of habitats at different scales using remote sensing and GIS methods. *Landscape and Urban Planning*, 67, 43–65.
- Weis, J. S., Edwards, J., Enger, E. D., Gall, G. A., Jarder, H. J., Lauritsen, D. D., et al. (2002). Biology, environment, and conservation in South Africa. *BioScience*, 52, 781–789.
- Wolmer, W. (2003). Transboundary conservation: The politics of ecological integrity in the Great Limpopo Transfrontier Park. *Journal of Southern African Studies*, 29, 261–278.